Nonlinear Interactions between Electromagnetic Waves and Electron Plasma Oscillations in Quantum Plasmas

P. K. Shukla* and B. Eliasson

Institut für Theoretische Physik IV, Fakultät für Physik und Astronomie, Ruhr-Universität Bochum, D-44780 Bochum, Germany; Department of Physics, Umeå University, SE-90187 Umeå, Sweden; and School of Physics, University of KwaZulu-Natal, 4000 Durban, South Africa

(Received 14 March 2007; published 30 August 2007)

We consider nonlinear interactions between intense circularly polarized electromagnetic (CPEM) waves and electron plasma oscillations (EPOs) in a dense quantum plasma, taking into account the electron density response in the presence of the relativistic ponderomotive force and mass increase in the CPEM wave fields. The dynamics of the CPEM waves and EPOs is governed by the two coupled nonlinear Schrödinger equations and Poisson's equation. The nonlinear equations admit the modulational instability of an intense CPEM pump wave against EPOs, leading to the formation and trapping of localized CPEM wave pipes in the electron density hole that is associated with a positive potential distribution in our dense plasma. The relevance of our investigation to the next generation intense laser-solid density plasma interaction experiments is discussed.

DOI: 10.1103/PhysRevLett.99.096401 PACS numbers: 71.10.Ca, 52.35.Sb, 71.15.Rf, 73.20.Mf

Studies of collective interactions in dense quantum plasmas is gaining momentum, although its foundation was laid down by Pines [1], who discussed the properties of electron plasma oscillations (EPOs) in a dense Fermi plasma. The high-density, low-temperature quantum Fermi plasma is significantly different from the low-density, high-temperature "classical plasma" obeying the Maxwell-Boltzmann distribution. In a very dense quantum plasma, there are new equations of state [2–4] associated with the Fermi-Dirac plasma particle distribution function and there are new quantum forces involving the quantum Bohm potential [5] and the electron-$1/2$ spin effect [6] due to magnetization. It should be noted that very dense quantum plasmas exist in intense laser-solid density plasma interaction experiments [7–9], in laser-based inertial fusion [10], in astrophysical and cosmological environments [11–13], and in quantum diodes [14].

It has been recently recognized [15–17] that quantum mechanical effects play an important role in intense laser-solid density plasma interaction experiments. In the latter, there are nonlinearities [18] associated with the electron mass increase in the electromagnetic (EM) fields and the modification of the electron number density by the relativistic ponderomotive force. Relativistic nonlinear effects in a classical plasma is very important, because they provide the possibility of the compression and localization of intense electromagnetic waves. In this Letter, we consider nonlinear interactions between intense circularly polarized electromagnetic (CPEM) waves and EPOs in dense quantum plasmas, which are relevant for a variety of applications in laboratories [8,9]. Specifically, in the following, we present theoretical and simulation studies of the CPEM wave modulational instability against EPOs, as well as the trapping of localized CPEM waves into a quantum electron hole in very dense quantum plasmas.

We consider a one-dimensional geometry of an unmagnetized dense electron-ion plasma, in which immobile ions form the neutralizing background. Thus, we are investigating the phenomena on a time scale shorter than the ion plasma period. Our dense quantum plasma contains an intense CPEM plane wave that nonlinearly interacts with EPOs. The nonlinear interaction between intense CPEM waves and EPOs gives rise to an envelope of the CPEM vector potential $\mathbf{A}_\perp = A_\perp(\hat{\mathbf{x}} + i\hat{\mathbf{y}})\exp(-i\omega_0 t + ik_0 z)$, which obeys the nonlinear Schrödinger equation [19]

$$2i\Omega_0\left(\frac{\partial}{\partial t} + V_g\frac{\partial}{\partial z}\right)A_\perp + \frac{\partial^2 A_\perp}{\partial z^2} - \left(\frac{|\psi|^2}{\gamma} - 1\right)A_\perp = 0, \tag{1}$$

where the electron wave function ψ and the scalar potential are governed by, respectively,

$$iH\frac{\partial\psi}{\partial t} + \frac{H^2}{2}\frac{\partial^2\psi}{\partial z^2} + (\phi - \gamma + 1)\psi = 0, \tag{2}$$

and

$$\frac{\partial^2\phi}{\partial z^2} = |\psi|^2 - 1, \tag{3}$$

where $\Omega_0 = \omega_0/\omega_{\rm pe}$, $V_g = v_g/c$, $H = \hbar\omega_{\rm pe}/mc^2$, $v_g = k_0c^2/\omega_0$ is the group velocity of the CPEM waves, and $\gamma = (1 + |A_\perp|^2)^{1/2}$ is the relativistic gamma factor due to the electron quiver velocity in the CPEM wave fields. Furthermore, $\omega_0 = (k_0^2c^2 + \omega_{\rm pe}^2)^{1/2}$ is the CPEM wave frequency, k_0 is the wave number, c is the speed of light in vacuum, $\omega_{\rm pe} = (4\pi n_0 e^2/m)^{1/2}$ is the electron plasma frequency, e is the magnitude of the electron charge, n_0 is the equilibrium electron number density, and m is the electron rest mass. In (1)–(3) the time and space variables are normalized by the inverse electron plasma frequency

$\omega_{\rm pe}^{-1}$ and skin depth $\lambda_e = c/\omega_{\rm pe}$, respectively, the scalar potential ϕ by mc^2/e, the vector potential $A_\perp$ by mc^2/e, and the electron wave function $\psi(z,t)$ by $n_0^{1/2}$. The nonlinear coupling between intense CPEM waves and EPOs comes about due to the nonlinear current density, which is represented by the term $|\psi|^2 A_\perp/\gamma$ in Eq. (1). The electron number density is defined as $n_e = \psi\psi^* = |\psi|^2$, where the asterisk denotes the complex conjugate. In Eq. (2), $1-\gamma$ is the relativistic ponderomotive potential [19], which arises due to the cross-coupling between the CPEM wave-induced electron quiver velocity and the CPEM wave magnetic field. The second term in the left-hand side in (2) is associated with the quantum Bohm potential [5].

It is well known [19] that a relativistically strong electromagnetic wave in a classical electron plasma is subjected to the Raman scattering and modulational instabilities. At quantum scales, these instabilities will be modified by the dispersive effects caused by the tunnelling of the electrons. In order to investigate the quantum mechanical effects on the relativistic parametric instabilities in a dense quantum plasma in the presence of a relativistically strong CPEM pump wave, we let $\phi(z,t) = \phi_1(z,t)$, $A_\perp(z,t) = [A_0 + A_1(z,t)]\exp(-i\alpha_0 t)$ and $\psi(z,t) = [1+\psi_1(z,t)]\exp(-i\beta_0 t)$, where A_0 is the large-amplitude CPEM pump and A_1 is the small-amplitude fluctuations of the CPEM wave amplitude due to the nonlinear coupling between CPEM waves and EPOs, i.e. $|A_1| \ll |A_0|$, and ψ_1 ($\ll 1$) is the small-amplitude perturbations in the electron wave function. The constant frequency shifts, determined from Eqs. (1) and (2), are $\alpha_0 = (1/\gamma_0 - 1)/(2\Omega_0)$ and $\beta_0 = (1-\gamma_0)/H$, where $\gamma_0 = (1+|A_0|^2)^{1/2}$. The first-order perturbations in the electromagnetic vector potential and the electron wave function are expanded into their respective sidebands as $A_1(z,t) = A_+\exp(iKz - i\Omega t) + A_-\exp(-iKz + i\Omega t)$ and $\psi_1(z,t) = \psi_+\exp(iKz - i\Omega t) + \psi_-\exp(-iKz + i\Omega t)$, while the potential is expanded as $\phi(z,t) = \hat{\phi}\exp(iKz - i\Omega t) + \hat{\phi}^*\exp(-iKz + i\Omega t)$, where Ω and K are the frequency and wave number of the electron plasma oscillations, respectively. Inserting the above mentioned Fourier ansatz into Eqs. (1)–(3), linearizing the resultant system of equations, and sorting into equations for different Fourier modes, we obtain the nonlinear dispersion relation

$$1 - \left(\frac{1}{D_+} + \frac{1}{D_-}\right)\left(1 + \frac{K^2}{D_L}\right)\frac{|A_0|^2}{2\gamma_0^3} = 0, \qquad (4)$$

where $D_\pm = \mp 2\Omega_0(\Omega - V_g K) + K^2$ and $D_L = 1 + H^2K^4/4 - \Omega^2$. We note that $D_L = 0$ yields the linear dispersion relation $\Omega^2 = 1 + H^2K^4/4$ for the EPOs in a dense quantum plasma [1]. For $H \to 0$ we recover from (4) the nonlinear dispersion relation for relativistically large-amplitude electromagnetic waves in a classical electron plasma [19]. The dispersion relation (4) governs the Raman backward and forward scattering instabilities, as well as the modulational instability. In the long-wavelength limit $V_g \ll 1$, $\Omega_0 \approx 1$ we introduce the ansatz $\Omega = i\Gamma$, where the normalized (by $\omega_{\rm pe}$) growth rate $\Gamma \ll 1$, and obtain from Eq. (4) the growth rate $\Gamma = (1/2)|K|\{(|A_0|^2/\gamma_0^3)[1 + K^2/(1 + H^2K^4/4)] - K^2\}^{1/2}$ of the modulational instability. For $|K| < 1$ and $H < 1$, the linear growth rate is only weakly depending on the quantum parameter H. However, possible nonlinear saturation of the modulational instability may lead to localized CPEM wave packets, which are trapped in a quantum electron hole. Such localized electromagnetic wave packets would have length scales much shorter than those involved in the modulational instability process. Here quantum diffraction effects (associated with the quantum Bohm potential) become very important. In order to investigate the quantum diffraction effect on such localized electromagnetic pulses, we consider a steady state structure moving with a constant speed V_g. Inserting the ansatz $A_\perp = W(\xi)\exp(-i\Omega t)$, $\psi = P(\xi)\exp(ikx - i\omega t)$ and $\phi = \phi(\xi)$ into Eqs. (1)–(3), where $\xi = z - V_g t$, $k = V_g/H$, and $\omega = V_g^2/2H$, and where $W(\xi)$ and $P(\xi)$ are real, we obtain from (1)–(3) the coupled system of equations

$$\frac{\partial^2 W}{\partial \xi^2} + \left(\lambda - \frac{P^2}{\gamma} + 1\right)W = 0, \qquad (5)$$

$$\frac{H^2}{2}\frac{\partial^2 P}{\partial \xi^2} + (\phi - \gamma + 1)P = 0, \qquad (6)$$

where $\gamma = (1+W^2)^{1/2}$, and

$$\frac{\partial^2 \phi}{\partial \xi^2} = P^2 - 1, \qquad (7)$$

with the boundary conditions $W = \Phi = 0$ and $P^2 = 1$ at $|\xi| = \infty$. In Eq. (5), $\lambda = 2\Omega_0\Omega$ represents a nonlinear frequency shift of the CPEM wave. In the limit $H \to 0$, we have from (6) $\phi = \gamma - 1$, where $P \neq 0$, and we recover the classical (nonquantum) case of the relativistic solitary waves in a cold plasma [20]. We note that the system of Eqs. (5)–(7) admits a Hamiltonian

$$Q_H = \frac{1}{2}\left(\frac{\partial W}{\partial \xi}\right)^2 + \frac{H^2}{2}\left(\frac{\partial P}{\partial \xi}\right)^2 - \frac{1}{2}\left(\frac{\partial \phi}{\partial \xi}\right)^2 + \frac{1}{2}(\lambda + 1)W^2 + P^2 - \gamma P^2 + \phi P^2 - \phi = 0, \qquad (8)$$

where we have used the boundary conditions $\partial/\partial\xi = 0$, $W = \phi = 0$, and $|P| = 1$ at $|\xi| = \infty$.

In order to asses the importance of our investigation, we now present numerical solutions of (1)–(3) and (5)–(7), ensuring that (8) is conserved. We chose parameters that are representative of the next generation laser-based plasma compression (LBPC) schemes [9,10]. The formula [18] $eA_\perp/mc^2 = 6\times 10^{-10}\lambda_s\sqrt{I}$ will determine the normalized vector potential, provided that the CPEM wavelength λ_s (in microns) and intensity I (in $\mathrm{W/cm^2}$) are

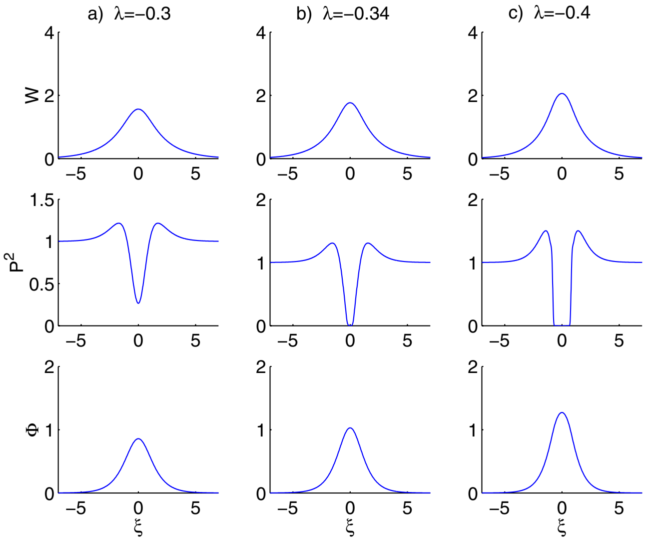

FIG. 1 (color online). The profiles of the CPEM vector potential $A_\perp$, the electron number density, and the scalar potential (upper to lower rows of panels) for $\lambda = -0.3$, $\lambda = -3.4$, and $\lambda = -0.4$, with $H = 0.002$.

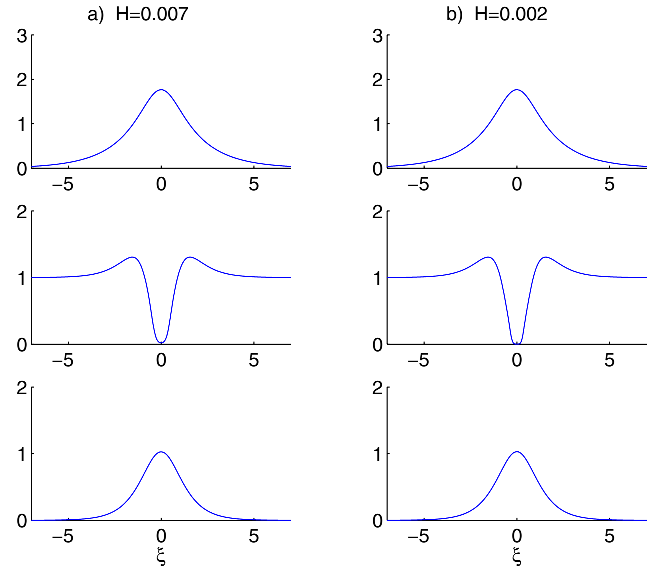

FIG. 2 (color online). The profiles of the CPEM vector potential $A_\perp$, the electron number density, and the scalar potential (upper to lower rows of panels) for $H = 0.007$ and $H = 0.002$, with $\lambda = -0.34$.

known. It is expected that in LBPC schemes, the electron number density n_0 may reach 10^{27} cm^{-3} and beyond, and the peak values of $eA_\perp/mc^2$ may be in the range 1–2 (e.g., for focused EM pulses with $\lambda_s \sim 0.15$ nm and $I \sim 5 \times 10^{27}$ W/cm^2). For $\omega_{\rm pe} = 1.76 \times 10^{18}$ s^{-1}, we have $\hbar\omega_{\rm pe} = 1.76 \times 10^{-9}$ erg and $H = 0.002$, since $mc^2 = 8.1 \times 10^{-7}$ erg. The electron skin depth $\lambda_e \sim 1.7$ Å. On the other hand, a higher value of $H = 0.007$ is achieved for $\omega_{\rm pe} = 5.64 \times 10^{18}$ s^{-1}. Thus, our numerical solutions below, based on these two values of H, have focused on scenarios that are relevant for the next generation intense laser-solid density plasma interaction experiments [9].

We first numerically solved Eqs. (5)–(7) for several values of H. Here, we solved the nonlinear boundary value problem with the boundary conditions $W = \phi = 0$ and $P = 1$ at the boundaries at $\xi = \pm 10$. We used centered second-order approximations for the second derivatives and solved the obtained nonlinear system of equations numerically by using the Newton method. The results are displayed in Figs. 1 and 2. We see that the solitary envelope pulse is composed of a single maximum of the localized vector potential W and a local depletion of the electron density P^2, and a localized positive potential ϕ at the center of the solitary pulse. The latter has a continuous spectrum in λ, where larger values of negative λ are associated with larger amplitude solitary EM pulses. At the center of the solitary EM pulse, the electron density is partially depleted, as in panels (a) of Fig. 1, and for larger amplitudes of the EM waves we have stronger depletion of the electron density, as shown in panels (b) and (c) of Fig. 1. For cases where the electron density goes to almost zero in the classical case [20], one important quantum effect is that the electrons can tunnel into the depleted region. This is seen in Fig. 2, where the electron density remains nonzero for the larger value of H in panels (a), while the density shrinks to zero for the smaller value of H in panel (b).

In order to investigate the quantum diffraction effects on the dynamics of localized CPEM wave packets, we have solved the system of Eqs. (1)–(3) numerically. We considered the long-wavelength limit $\omega_0 \approx 1$ and $V_g \approx 0$. In the initial conditions, we use an EM pump with a constant amplitude $A_\perp = A_0 = 1$ and a uniform plasma density

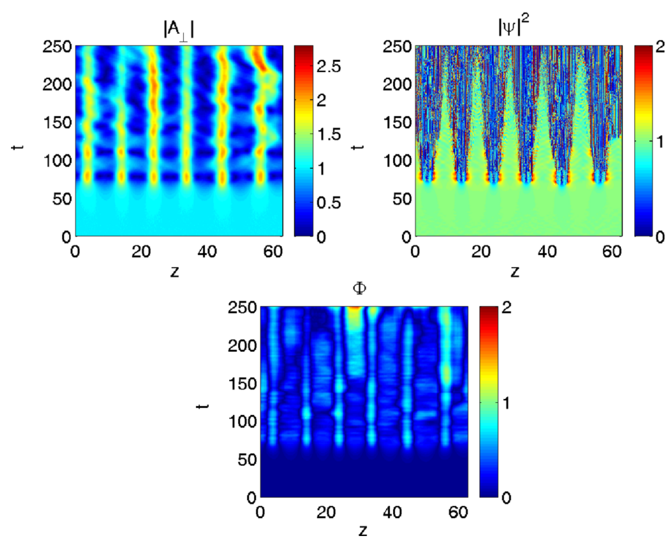

FIG. 3 (color online). The dynamics of the CPEM vector potential $A_\perp$ and the electron number density $|\psi|^2$ (upper panels) and of the electrostatic potential Φ (lower panel) for $H = 0.002$.

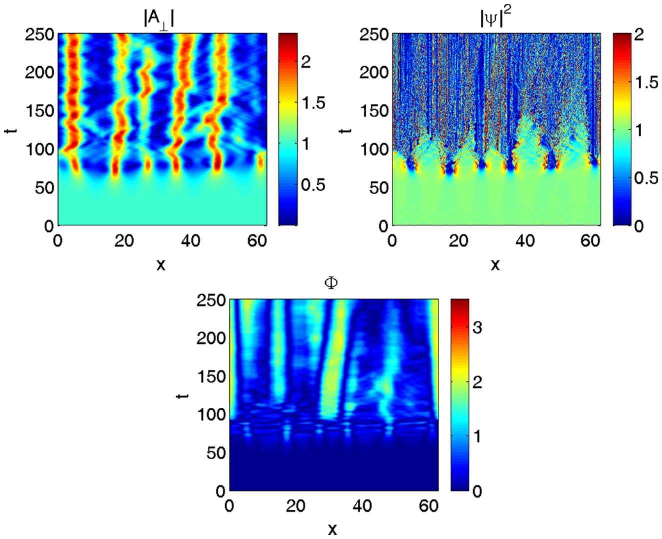

FIG. 4 (color online). The dynamics of the CPEM vector potential $A_\perp$ and the electron number density $|\psi|^2$ (upper panels) and the electrostatic potential ϕ (lower panel) for $H = 0.007$.

$\psi = 1$. A small-amplitude noise (random numbers) of order 10^{-2} is added to $A_\perp$ to give a seed for any instability. The numerical results are displayed in Figs. 3 and 4 for $H = 0.002$ and $H = 0.007$, respectively. In both cases, we see an initial linear growth phase and a wave collapse at $t \approx 70$, in which almost all the CPEM wave energy is contracted into a few well-separated localized CPEM wave pipes. These are characterized by a large bell-shaped amplitude of the CPEM wave, an almost complete depletion of the electron number density at the center of the CPEM wave packet, and a large-amplitude positive electrostatic potential. Comparing Fig. 3 with Fig. 4, we see that there is a more complex dynamics in the interaction between the CPEM wave packets for the larger $H = 0.007$, shown in Fig. 4, in comparison with $H = 0.002$, shown in Fig. 3, where the wave packets are almost stationary when they are fully developed. We have here neglected the effects of the ion dynamics. The latter may be important for the development of expanding plasma bubbles (cavities) on longer time scales (e.g., the ion plasma period) [21].

In conclusion, we have presented theoretical and computer simulation studies of nonlinearly interacting intense CPEM waves and EPOs in very dense quantum plasmas. Specifically, we have identified a new modulational instability of an arbitrary large-amplitude CPEM due to the quantum diffraction effect that is controlled by the parameter H. Our simulation results reveal that the parameter H plays a crucial role in the formation of localized intense CPEM pulses, which are trapped in a quantum electron hole at nanoscales. The localized CPEM wave structures, as discussed here, may be useful for information transfer as well as for electron acceleration in dense quantum plasmas, such as those in the next generation intense laser-solid density plasma interaction experiments.

This work was supported by the DFG through the SFB 591, and by the Swedish Research Council (VR).

*Also at SUPA Department of Physics, University of Strathclyde, Glasgow G4 0NG, United Kingdom and Instituto Superior T, USAécnico, Universidade Técnica de Lisboa, 1049-001 Lisboa, Portugal.

[1] D. Pines, J. Nucl. Energy, Part C, Plasma Phys. Accel. Thermonucl. Res. **2**, 5 (1961).
[2] G. Manfredi and F. Haas, Phys. Rev. B **64**, 075316 (2001).
[3] G. Manfredi, Fields Inst. Commun. **46**, 263 (2005).
[4] P. K. Shukla and B. Eliasson, Phys. Rev. Lett. **96**, 245001 (2006).
[5] C. L. Gardner and C. Ringhofer, Phys. Rev. E **53**, 157 (1996).
[6] M. Marklund and G. Brodin, Phys. Rev. Lett. **98**, 025001 (2007).
[7] S. X. Hu and C. H. Keitel, Phys. Rev. Lett. **83**, 4709 (1999); Y. A. Salamin *et al.*, Phys. Rep. **427**, 41 (2006).
[8] S. H. Glenzer *et al.*, Phys. Rev. Lett. **98**, 065002 (2007).
[9] V. M. Malkin *et al.*, Phys. Rev. E **75**, 026404 (2007).
[10] H. Azechi *et al.*, Plasma Phys. Controlled Fusion **48**, B267 (2006).
[11] M. Opher *et al.*, Phys. Plasmas **8**, 2454 (2001).
[12] O. G. Benvenuto and M. A. De Vito, Mon. Not. R. Astron. Soc. **362**, 891 (2005).
[13] G. Chabrier *et al.*, J. Phys. Condens. Matter **14**, 9133 (2002); J. Phys. A **39**, 4411 (2006).
[14] Y. Y. Lau *et al.*, Phys. Rev. Lett. **66**, 1446 (1991); L. K. Ang *et al.*, *ibid.* **91**, 208303 (2003); L. K. Ang and P. Zhang, *ibid.* **98**, 164802 (2007).
[15] A. V. Andreev, JETP Lett. **72**, 238 (2000).
[16] G. Mourou *et al.*, Rev. Mod. Phys. **78**, 309 (2006).
[17] M. Marklund and P. K. Shukla, Rev. Mod. Phys. **78**, 591 (2006).
[18] P. K. Shukla *et al.*, Phys. Rep. **138**, 1 (1986).
[19] C. J. McKinstrie and R. Bingham, Phys. Fluids B **4**, 2626 (1992).
[20] J. H. Marburger and R. F. Tooper, Phys. Rev. Lett. **35**, 1001 (1975).
[21] M. Borghesi *et al.*, Phys. Rev. Lett. **88**, 135002 (2002).